

# Petrography and geochemistry of the Golero's Rhyolite Unit north of Valledupar city, Cesar, Colombia

## Petrografía y geoquímica de la Unidad Riolita de Golero al norte de la ciudad de Valledupar, Cesar, Colombia

Elías Ernesto Rojas Martínez<sup>1</sup>, Dino Carmelo Manco-Jaraba<sup>2\*</sup>, Frank David Lascarro-Navarro<sup>3</sup>, Libardo Lascarro-Navarro<sup>4</sup>, Luis Gutiérrez-Pacheco<sup>5</sup>, Carlos Alberto Ríos-Reyes<sup>6</sup>

1. Geólogo, Magister en Geología Económica, Fundación Universitaria del Área Andina. E-mail: eliaser@hotmail.com  
ORCID: <https://orcid.org/0000-0003-0402-1565>
2. Ingeniero de Minas, M.Sc. Gestión Ambiental y Energética en las Organizaciones, Universidad de La Guajira. E-mail: dinomancojaraba@gmail.com,  
ORCID: <https://orcid.org/0000-0001-8506-094X>
3. Ingeniero geólogo, Universidad Nacional Mayor de San Marcos. E-mail: frank.lascarro@unmsm.edu.pe  
ORCID: <https://orcid.org/0000-0001-9433-2863>
4. Geólogo, Universidad de Pamplona. E-mail: Libardo.lascarronavarro@gmail.com ORCID: <https://orcid.org/0000-0002-1891-034X>
5. Ingeniero geólogo, Fundación Universitaria del Área Andina. E-mail: Luis.gutierrez@tctgamas.com ORCID: <https://orcid.org/0000-0002-2014-1201>
6. Geólogo, Doctor en Ciencias Aplicadas, Universidad Industrial de Santander. E-mail: carios@uis.edu.co  
ORCID: <https://orcid.org/0000-0002-3508-0771>

Cite this article as: E. E. Rojas-Martínez, D. C. Manco-Jaraba, F. D. Lascarro-Navarro, L. Lascarro-Navarro, L. Gutiérrez-Pacheco, C. A. Ríos-Reyes "Petrography and geochemistry of the Golero's Rhyolite Unit north of Valledupar city, Cesar, Colombia", *Prospectiva*, Vol. 22 N° 2 2024.

Recibido: 27/09/2023 / Aceptado: 01/04/2024

<http://doi.org/10.15665/rp.v22i2.3301>

### ABSTRACT

*The Golero's Rhyolite is a lithological unit of heterogeneous composition, consisting of basaltic, dacitic, andesitic and rhyolitic volcanic rocks that outcrops on the eastern and southern flank of the Sierra Nevada de Santa Marta, northwestern tip of South America. The study area comprises the rural area north of Valledupar City, Cesar, Colombia. The objective of this re-search is to analyze petrographically and geochemically the volcanic rocks of the Golero's Rhyolite Unit north of the city of Valledupar, Cesar, Colombia. For the execution of the research, we initially proceeded with a compilation of cartographic information at a scale of 1:25,000, where lithological and structural characteristics were identified; later, field trips and collection of 22 samples for compositional and textural classification, selecting 9 specimens for micropetrographic and geochemical analysis (X-ray fluorescence). Macroscopic and microscopic petrographic analysis evidences that they consist of aphanitic matrix composed mostly of plagioclase, with porphyritic inequigranular and sometimes bimodal inequigranular texture or grain size distribution, in general there are euhedral to subhedral plagioclase minerals, epidote altering the plagioclase, subhedral hornblende, subhedral feldspar, anhedral quartz, and in smaller proportion hematite, magnetite and calcite in veinlets. Within the element's variation diagrams the samples are located in the same crystallization sequence, suggesting that they are part of the same magmatism and fractionation of the rocks from SiO<sub>2</sub> values of 44.63 wt% to 63.07 wt %; (basalts to dacites). The rocks of the Golero's Rhyolite Unit were generated from a calc-alkaline magma in an intraplate tectonic environment, possibly influenced by oceanic islands arc (OIA) product of continental rifting.*

**Keywords:** *Geochemistry, Petrograph, Rhyolite of Golero, Tectonic environment.*

### RESUMEN

*La Riolita de Golero es una Unidad litológica de composición heterogénea, constituida por rocas volcánicas basálticas, dacíticas, andesíticas y riolíticas que aflora en el flanco oriental y sur de la Sierra Nevada de Santa Marta, extremo noroccidental de Suramérica. El área de estudio comprende la zona rural al norte del municipio de Valledupar, Cesar, Colombia. El objetivo de esta investigación es analizar Petrográfica y geoquímicamente las rocas volcánicas de la Unidad Riolita de Golero al norte de la ciudad de Valledupar, Cesar, Colombia. Para la ejecución de la investigación se procedió inicialmente con una recopilación de información cartográfica a escala 1:25.000, donde se identificaron características litológicas y estructurales; posteriormente, salidas de campo y toma de 22 muestras para clasificación composicional y textural, seleccionándose 9 especímenes para análisis micropetrográfico y geoquímico (fluorescencia de rayos X). Los análisis petrográficos macroscópicos y microscópicos evidencian que están constituidas por matriz afanítica compuesta en su mayoría por plagioclasas, con textura o distribución de tamaño de grano inequigranular porfídica y en ocasiones inequigranular bimodal, en general se encuentra minerales de plagioclasa euhedral a subhedral, epidota alterando la plagioclasa, hornblenda subhedral, feldespato subhedral, cuarzo anhedral, y en menor proporción hematita, magnetita y calcita*

*en vetillas. Dentro de los diagramas de variación elementales las muestras se localizan en la misma secuencia de cristalización, sugiriendo que hacen parte del mismo magmatismo y fraccionamiento de las rocas desde valores en SiO<sub>2</sub> de 44.63 wt% hasta 63.07 wt %; (basaltos a dacitas). Las rocas volcánicas de la Unidad Riolita del Golero, se generaron a partir de un magma calcoalcalino en un ambiente tectónico de intraplaca, posiblemente con influencia de arco de isla oceánica (OIA) producto de rift continental.*

**Palabras clave:** *Ambiente tectónico, Geoquímica, Petrografía, Riolita de Golero.*

---

## 1. INTRODUCTION

The Sierra Nevada Massif (SNSM) constitutes an isolated mountain system of Los Andes located in the northwestern corner of South America (Fig. 1). It is characterized by a very complex tectonic configuration due to the interaction between the South American continental plate and the Caribbean and Nazca oceanic plates [1], [2]. The Caribbean Continental Margin and the Caribbean Plate were formed in the Late Cretaceous, the tectonic events that have demarcated the position and current tectonic configuration of the SNSM date from the Oligocene to the Pliocene [3]–[5].

One of the most outstanding events in the SNSM is the extensive magmatic activity that took place in the Triassic and Jurassic periods, accompanied by large volumes of volcanic and volcanoclastic rocks. During the early to middle Jurassic, the extensive magmatic arc that occurred in the SNSM generated two very large belts of granitoids. The first one occurred in the SNSM towards the central part with intermediate composition and the other towards the southern part of acid composition [6]–[8]. These granitoids were accompanied by the development of a back-arc basin with abundant volcanic and volcanoclastic rocks southeast of the SNSM [9]–[11]. The intense magmatism in much of the Norandina region is explained by two models: the first states that this intrusive and effusive igneous activity is the product of the subduction of an oceanic plate under the South American plate [12], [13]. The second one proposes cortical thinning, bulging of the mantle and a zone of supracontinental distension [14], [15].

The SNSM is divided into three geological provinces from northwest to southeast: the first is the Province of Santa Marta, composed of two metamorphic belts of Perm-Triassic schists and amphibolites [16], [17] and Cretaceous phyllites [18], separated by an Eocene tonalitic intrusive, the Santa Marta Batolith [19]–[21]. The second province is the Province of Seville, composed of ortho- and paragneisses whose age of metamorphism is associated with the Late Paleozoic and which forms a NE-SW belt [21], [22]. And finally, a third province, the Sierra Nevada Province, composed mainly of a Mesoproterozoic metamorphic basement intruded by extensive Jurassic granitoids; towards the most southeastern part of this province there is a margin of volcanic and volcanoclastic rocks, which are overlain by sedimentary rocks from the Cretaceous and the Cenozoic [21], [23]. In this last province, the study area is located geologically.

The study area (Fig. 1) corresponds to a strip of 40 km<sup>2</sup>, located on the eastern flank of the SNSM, north of the department of Cesar, approximately 4 km NW of the City of Valledupar. In this sector, a volcanic unit of acidic to intermediate composition with interposition of associated volcanoclastic rocks (Ignimbrite and tuffs), known as the Golero's Rhyolite, on the south and eastern flanks of the SNSM, appears in an area of approximately 25 km<sup>2</sup> [7]–[9]. The present work represents the first report that describes and establishes a relationship between the petrography and geochemistry of the Golero's Rhyolite, north of the city of Valledupar, providing new data on this geological unit of great importance in the understanding of the genesis of volcanic sequences in the geotectonic context of the SNSM.

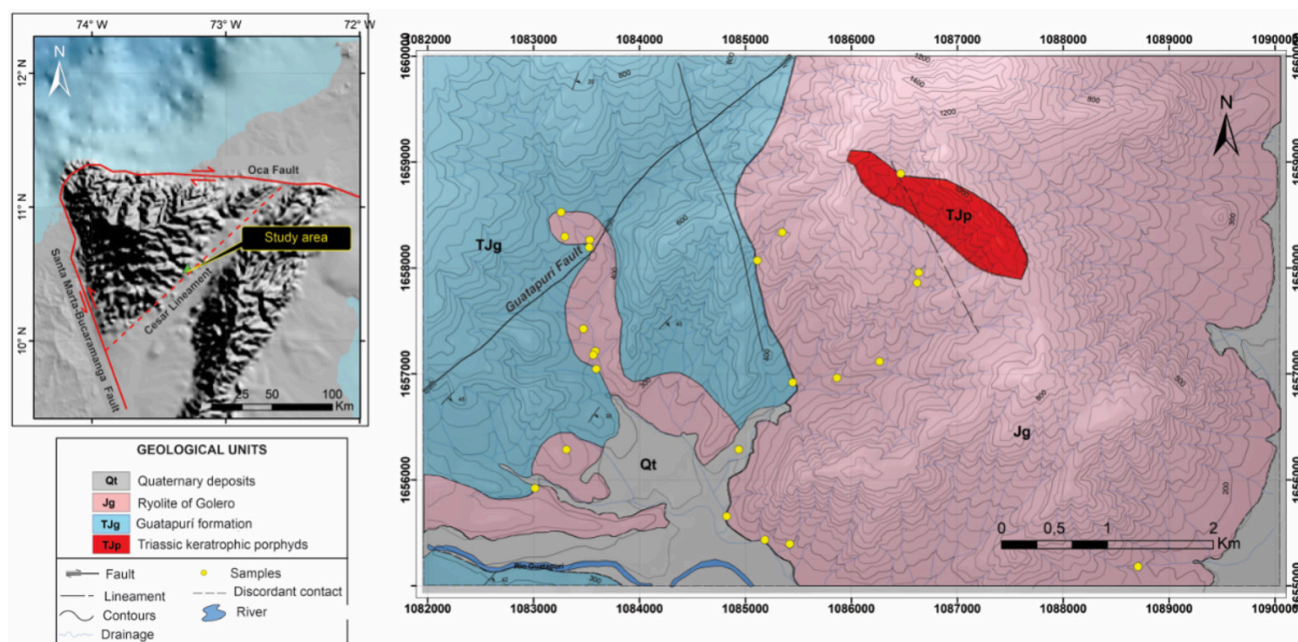


**Figure 1.** Location of area of study. In this the geology and sampling sites are observed.

## 2. REGIONAL AND LOCAL GEOLOGICAL FRAMEWORK

Colmenares [10], describe the Golero's Rhyolite as a succession of volcanic rocks of acidic to intermediate composition that present different textures such as porphyritic, porphyriafanitic and aphanitic. It presents interposition levels of associated volcanoclastic rocks such as ignimbrites and tuffs, pyroclastic fragments. These rocks are highly weathered product of water flows and wind [24], [25]. The Golero's Rhyolite is considered the only Cretaceous volcanic unit present in the Sierra Nevada de Santa Marta [26], this being the most recent volcanic unit of age Kimmeridgian - Hauterivian, with K/Ar dates of  $152.9 \pm 4.0$  Ma for the area of Valledupar and of  $128.2 \pm 2.7$  Ma, for the area of the municipality of Bosconia [7]–[9]. Tschanz [7], [8], report that this is the product of vesiculation of the porphyry granite magma, of the last differentiation of the Jurassic magmatic series. Likewise [26] include the Golero's Rhyolite with the rhyolitic rocks of the Upper Jurassic due to their common origin as the final product of a process of magmatic differentiation that begins in the early Jurassic. The contacts of this unit are reported as discordant on the plutonic, volcanic, volcanoclastic and older sedimentary units belonging to the Atanquez Batholith, Patillal Batholith, Guatapuri Formation and Los Clavos's Ignimbrite [10].

## 3. METHODS

In the present study, activities of compilation of cartographic information at a scale of 1:25.000 were performed, where lithological and structural features were identified, as well as field relations with other outcropping units. A sample was made where 22 samples were obtained for compositional and textural classification, of which 9 were selected for their microscopic analysis from the count of 300 points per thin section, following the methodology of [27]. The abbreviations of the minerals are according to [28]. The petrographic analyzes were carried out in the laboratory of the Fundación Universitaria del Area Andina, Valledupar; the oxides and trace elements chemical analyze were carried out in the X-ray fluorescence spectrometer, MagixPro PW-2440 Philips (WDXRF) equipped with a Rhodium tube, with a maximum power of 4 KW of the X-Ray Fluorescence Laboratory of the National University of Colombia. This equipment has a sensitivity of 100ppm (0.01%) in the detection of heavy metallic elements. The preparations of the samples were mechanically perpetrated, first reduced with an agate ball mill, and then passed through a 100 $\mu$  mesh screen. The powder samples were dried at 105 °C, for a period of 12 hours. Later mixed with wax spectrometry in ratio Sample: Wax of 10: 1. This was homogenized by agitation, taken to a hydraulic press at 120 kN for one minute generating five pressed tablets of 37mm diameter that were measured in the SEMIQ-2017



application. The semi-quantitative analysis was carried out with the software SemiQ 5, doing 11 sweeps, in order to detect all the elements, present in the sample, excluding H, C, Li, Be, B, N, O and the transuranic elements.

## 4. RESULTS AND DISCUSSIONS

### 4.1 Lithologies and field relations

The outcrops are located north of the road that connects Valledupar with the village of Sabana Crespo, where there is a series of volcanic rocks and vulcanoclastics rocks in discordant contact with the Guatapuri Formation, Triassic Keratófiros porphyries and the recent deposits of the Quaternary (Geological Map 27 -Valledupar) [10]. In general, the rocks have porphyritic textures and some dark colored xenoliths of basaltic composition (Figs. 2a, 2b, 2c, 2d, 2e), and occasionally veinlets with minerals, such as calcite, quartz; abundant hematite and other iron oxides, which make the reddish-brown outcrops (Fig. 2f). The best outcrops that show the contacts with the Guatapuri Formation are exposed in the El Capitanejo stream, El Mamon stream and Aguas Blancas stream.

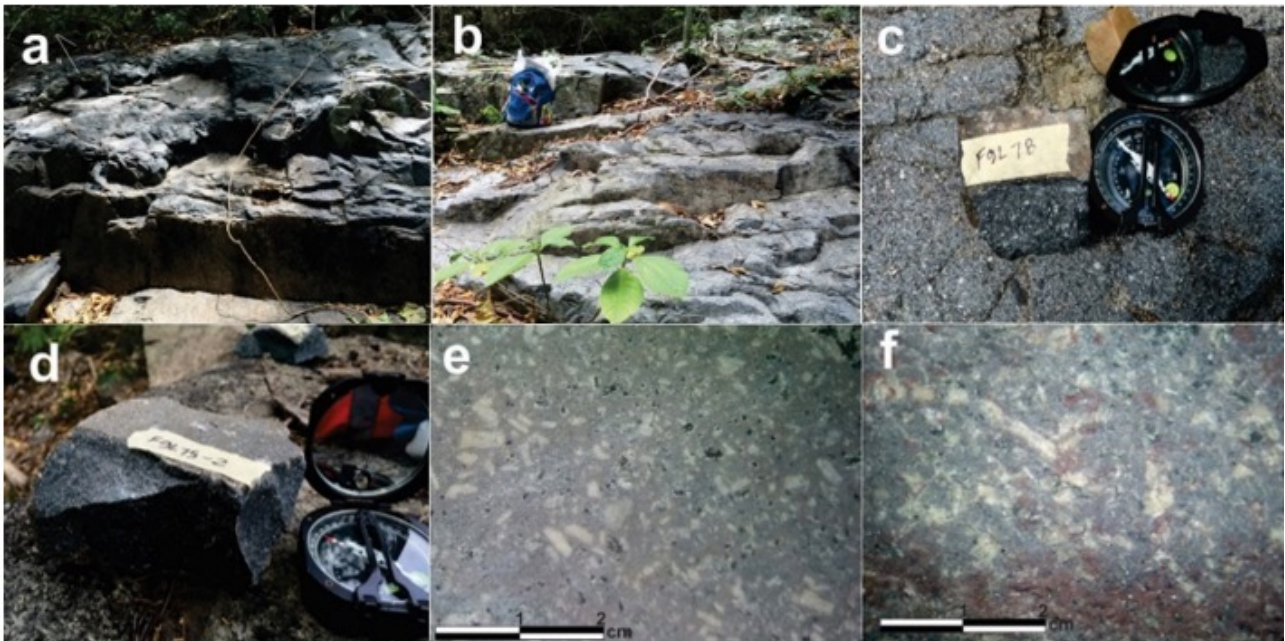


**Figure 2.** Outcrops of the Golero Rhyolite Unit, (a) - (b), with a very low level of weathering, with gray-to-gray tones greenish, (c) - (d). Photographs taken with stereoscope, where porphyritic textures are evidenced as well as iron oxides (hematite) filling small fractures (e) - (f).

### 4.2 Petrography

Figure 3, illustrates the microscopic scale classification of the volcanic rocks of the Golero's Rhyolite, according to the classification of [29]. The basalts are of dark greenish gray to bluish gray color, with an aphanitic matrix, with a degree of crystallinity greater than 90% in volume of crystals, holocrystalline, with an unequal porphyritic texture and sometimes unequal bimodal, in general euhedral plagioclases is found, epidote plagioclase, euhedral hornblende, subhedral feldspar, anhedral quartz and to a lesser extent hematite, magnetite and calcite veinlets.

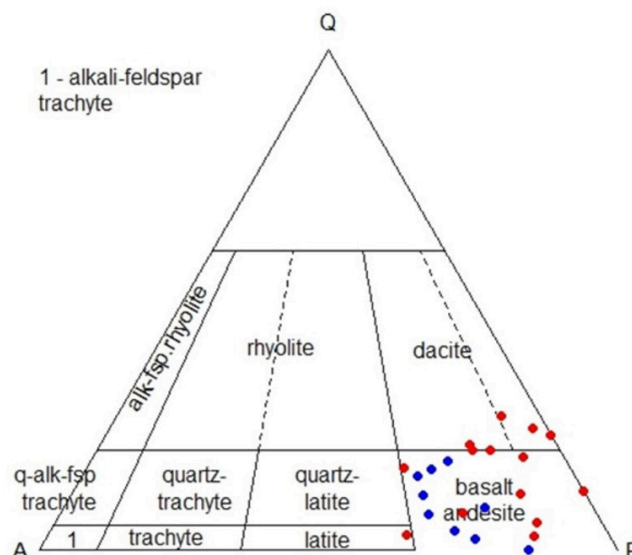


**Figure 3.** QAP classification diagram of [29], illustrating the compositional variations of the Golero's Rhyolite. The red and blue circles represent the rocks analyzed on a macroscopic scale and in a thin section, respectively.

The andesites are volcano-sedimentary (Ignimbrites), holocrystalline, of light greenish-gray color, of aphanitic matrix, with unequal bimodal grain size distribution, generally presenting anhedral quartz, subhedral feldspar, euhedral plagioclase, epidotized plagioclase, subhedral epidote, euhedral hornblende, biotite subhedral to euhedral, calcite in veinlets, in some cases hematite and magnetite; presents xenoliths of dark gray and light greenish gray, larger than 7 millimeters, usually of basic composition of aphanitic matrix.

The dacites are volcano-sedimentary, crystalline tuffs of intermediate composition, holocrystalline of dark gray color, of aphanitic matrix, with unequal grain size distribution and unequal bimodal, with anhedral quartz minerals, subhedral feldspar, euhedral plagioclase, epidotized plagioclase, euhedral hornblende, biotite subhedral to euhedral, and calcite in veinlets. The rocks present xenoliths of dark coloration, generally of basaltic composition.

The samples in the present study do not present directional textures, with disordered components, predominantly aphanitic and porphyritic textures, some xenoliths and extreme epidotization. The porphyritic texture indicates a two-stage cooling process with phenocrysts that grow slowly in a magmatic chamber in a very fine-grained matrix formed during rapid cooling at the earth's surface. Petrographically, these rocks vary in composition from andesitic to basaltic, with a high content of plagioclase (greater than 70%), quartz (not greater than 15%) and orthoclase (0-10%). Next, the main textural and microstructural features (Figs. 4 - 5) of the rocks analyzed are described.

The FGL 02 sample corresponds to an ignimbrite of andesitic composition (Figs. 4a-4b-4c), characterized by porphyritic texture with aphanitic matrix, phenocrysts mainly plagioclase labradorite and andesine in concentrations greater than or equal to 25%, quartz (15%) and hornblende (10%). The augite occurs locally in percentage less than 2%. Opaque minerals (possibly pyrite or chalcopyrite) have square contours and occur in less than 1%.

The sample FGL 7-1 corresponds to a basalt (Figs. 4d-4e-4f), characterized by a porphyritic texture with aphanitic matrix and predominance of plagioclase phenocrysts (30%) of intermediate composition (andesine) and quartz (5%). Opaque minerals of rounded contour are observed, possibly hematite and / or titanite-magnetite.

The sample FGL 7-2 corresponds to a porphyritic ignimbrite of andesitic composition (Figs. 4g-4h-4i), with porphyritic texture with aphanitic matrix, with phenocrysts mainly of plagioclase (42%) of intermediate composition (andesine) and quartz (5%). Plagioclase has undergone a strong epidotization, with development of zoisite, clinozoisite and epidote. Clinozoisites usually occur around altered plagioclase, bordering the phenocrysts.



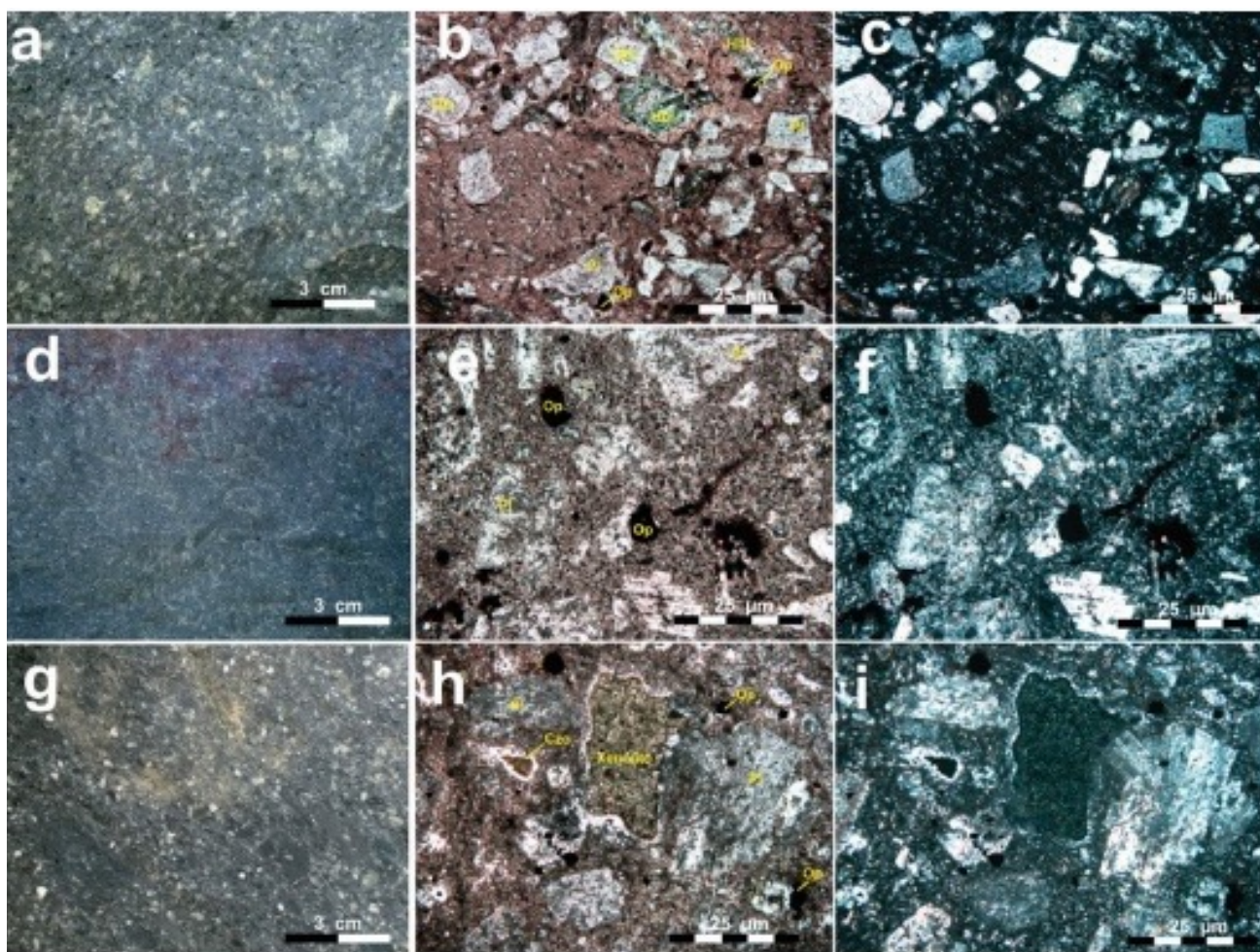


**Figure 4.** Macroscopic photographs (Left) and microphotographs in flat light not analyzed (Center) and plane light analyzed (right) of the samples (a), (b) y (c) FGL 02, (d), (e), (f) FGL 7-1 and (g), (h), (i) FGL 7-2.

The sample FGL 27 corresponds to a basalt (Figs. 5a-5b-5c), which presents a porphyritic texture with aphanitic matrix and phenocrysts (up to ~35%), represented by plagioclase (18%), hornblende (12%) and quartz (5%). Plagioclase occurs in tabular crystals with its characteristic polysynthetic twin. The hornblende develops locally a glomeroporphyritic texture, and is characterized to present pseudohexagonal outline, yellowish brown color with slight pleochroism and exfoliation in two directions. Calcite veinlets are locally observed.

The sample FGL 21 corresponds to a basalt (Figs. 5e-5f), with porphyritic texture, aphanitic matrix and phenocrysts (up to ~32%), represented by plagioclase (15%), hornblende (11%) and quartz (6%). Plagioclase shows a mild to marked epidotization. The hornblende is characterized by yellowish color with mild pleochroism and exfoliation in two directions. Hematite and possibly pyrite and/or chalcopyrite represent the main opaque minerals.

The FGL 30 sample corresponds to a calcoalkaline basalt (Figs. 5g-5h-5i), presents porphyritic texture with aphanitic matrix and phenocrysts (up to ~50%), represented by plagioclase (40%) and quartz (10%). An extensive distribution of hematite is observed in the interstices between plagioclase phenocrysts. Plagioclase shows epidotization, with development of clinozoisite and epidote. Opaque minerals show a square to slightly rounded contour.

Figure 5. Macroscopic photographs (left) and photomicrographs in flat light (Center) and po-larized light (right) of the samples (a), (b), (c) FGL 27, (d), (e), (f) FGL 21 and (g), (h), (i) FGL 30.

### 4.3 Geochemistry

For the geochemical study of the volcanic rocks of Golero's Rhyolite, nine (9) samples were selected to obtain the chemical composition of the major, minor and trace elements, in order to establish the nature of the magmatism and the tectonic context in which these rocks were formed. From the geochemical point of view, these samples correspond according to the TAS classification of Middlemost [30]1991 (Fig. 6), to Basalts, dacites and andesites.

Figure 6. TAS classification diagram of [30], illustrating the compositional variations of the Golero's Rhyolite according to X-ray fluorescence analysis (blue circles).

The chemical results of the samples in the different graphs were compared in order to determine if these were formed during the same igneous event, following the Harker variation diagrams [31] that establish how the concentration of SiO<sub>2</sub> increases with the magmatic evolution. In this way, the SiO<sub>2</sub> is projected on the abscissa against the remaining oxides in the ordinate (MgO, FeO, CaO, K<sub>2</sub>O, Al<sub>2</sub>O<sub>3</sub>, TiO<sub>2</sub>).

The Table 1 shows the geochemical results of each of the samples selected for FRX. According to the data of major elements, the SiO<sub>2</sub> contents vary between 44.63 wt% and 63.07 wt%; TiO<sub>2</sub> in general does not exceed 2.43 wt%, however concentrations around 0.8 wt% predominate; high values of K<sub>2</sub>O and Al<sub>2</sub>O<sub>3</sub> are presented between 1.91 and 3.85 wt% and 16.31 and 18.97 wt% respectively due to the large amount of iron oxides (hematite, magnetite), Fe<sub>2</sub>O<sub>3</sub> vary between 4.98 wt% and 13.71 wt%; Due to the low content of ferromagnesian minerals in acid rocks, the MgO varies from 2.24 wt% to 6.84 wt%, the CaO between 3.35 wt% to 7.69 wt%, the P<sub>2</sub>O<sub>5</sub> between 0.29 wt% to 0.86 wt% and the Na<sub>2</sub>O between 2.72 and 4.44 wt%.

**Table 1.** Results of the chemical analysis by the FRX technique. Oxides in wt% and elements in ppm.

Element and/or Oxides	M-F LG-02 (% Wt)	M-F LG-08 (% Wt)	M-F LG-11 (% Wt)	M-F LG-21 (% Wt)	M-F LG-26 (% Wt)	M-F GL7-2 (% Wt)	M-F GL-30 (% Wt)	M-F GL27-1 (% Wt)	M-FGL07 (% Wt)
SiO <sub>2</sub>	63.07%	44.63%	57.76%	62.30%	52.62%	62.69%	51.20%	53.47%	60.42%
Al <sub>2</sub> O <sub>3</sub>	16.59%	16.74%	16.31%	16.32%	18.97%	16.46%	16.53%	16.53%	16.45%
Fe <sub>2</sub> O <sub>3</sub>	4.98%	13.71%	6.89%	5.69%	9.33%	5.34%	10.30%	9.70%	5.94%
Na <sub>2</sub> O	4.43%	2.72%	4.44%	4.16%	3.63%	4.30%	3.58%	3.44%	4.44%
K <sub>2</sub> O	3.85%	1.00%	3.06%	2.81%	2.76%	3.33%	2.03%	1.91%	3.46%
CaO	3.35%	7.69%	5.10%	4.00%	7.34%	3.68%	6.40%	5.85%	4.23%
MgO	2.24%	9.48%	4.19%	3.07%	3.12%	2.66%	6.84%	6.28%	3.22%
TiO <sub>2</sub>	0.72%	2.43%	1.02%	0.88%	1.23%	0.80%	1.73%	1.66%	0.87%
P <sub>2</sub> O <sub>5</sub>	0.29%	0.86%	0.46%	0.37%	0.48%	0.33%	0.66%	0.62%	0.38%
MnO	0.14%	0.23%	0.11%	0.08%	0.14%	0.11%	0.17%	0.16%	0.13%
TOTAL	99.66%	99.49%	99.34%	99.68%	99.62%	99.67%	99.42%	99.59%	99.50%
Cl (ppm)	1200	1200	3800	900	800	1050	2500	1050	2500
Ba (ppm)	1200	1000	1100	700	1400	950	1050	850	1150
Sr (ppm)	500	500	600	500	700	500	550	500	550
Zr (ppm)	400	400	400	400	400	400	400	400	400
Rb (ppm)	200	20	84	60	69	0.0001	52	41	200
SO <sub>3</sub> (ppm)	100	400	200	0	0	100	300	200	150
Zn (ppm)	100	200	60	77	89	0.0001	67	100	100
V (ppm)	0	200	200	100	200	0	200	150	0
Ni (ppm)	0	100	0	0	0	0	100	100	0
Cr (ppm)	77	400	100	100	77	100	250	250	86
Cu (ppm)	65	200	69	200	62	100	100	200	100
Y (ppm)	37	28	32	33	38	35	27	30	39
Nb (ppm)	21	33	0	18	0	23	0	26	20

#### 4.4 Element variation diagrams

The variation diagrams of [32] allow through inter-elemental relationships to infer magmatic processes, as well as to infer more probable physicochemical conditions in which the fusion and crystallization processes are carried out, comparing natural compositions with experimental compositions obtained in pressure, temperature, and composition conditions well defined. It is inferred that the decrease of Fe and Ca oxides with the increase of SiO<sub>2</sub> would be consistent with the early removal of plagioclase, olivine and/or pyroxenes from the liquid that cools. It is deduced that its decrease is due to the fact that the FeO is incorporated in the mafic minerals of early formation, the CaO is incorporated to the calcium plagioclase and/or the pyroxene, while the MgO decrease is represented by the number of hornblendes and/or pyroxenes. The increase in K<sub>2</sub>O and Na<sub>2</sub>O is due to the fact that they are not incorporated into the minerals that crystallize and are conserved or concentrated in the residual liquid. The curves of Al<sub>2</sub>O<sub>3</sub>, CaO and Fe<sub>2</sub>O<sub>3</sub> decrease continuously, this can be interpreted by speculating that clinopyroxene separated early removing Ca



and Al, the plagioclase started to crystallize later taking Ca and not Al (Fig. 7). The rock samples from the Golero's Rhyolite Unit (in blue) are generally located within the same sequence or train of crystallization, suggesting that they are part of the same magmatism and fractionation of rocks from SiO<sub>2</sub> values of 44.63 wt% to 63.07 wt%; (basalts to dacites), with variations in the trends of the oxides as the SiO<sub>2</sub> content increases. However, [32] clarifies that as there are different systems that evolve in different ways (volcanic systems, stratified mafic intrusions, etc.), it should not be expected that a single parameter such as SiO<sub>2</sub>, can act equally well for all systems.

The lithological distribution found in the field shows a relationship with the geochemical evidences of the diagrams [32], suggesting that the different lithologies of the Golero Rhyolite Unit belong to the same pulse, generated by fractional crystallization [31], [33], starting with basalts and ending with dacites (Fig. 7).

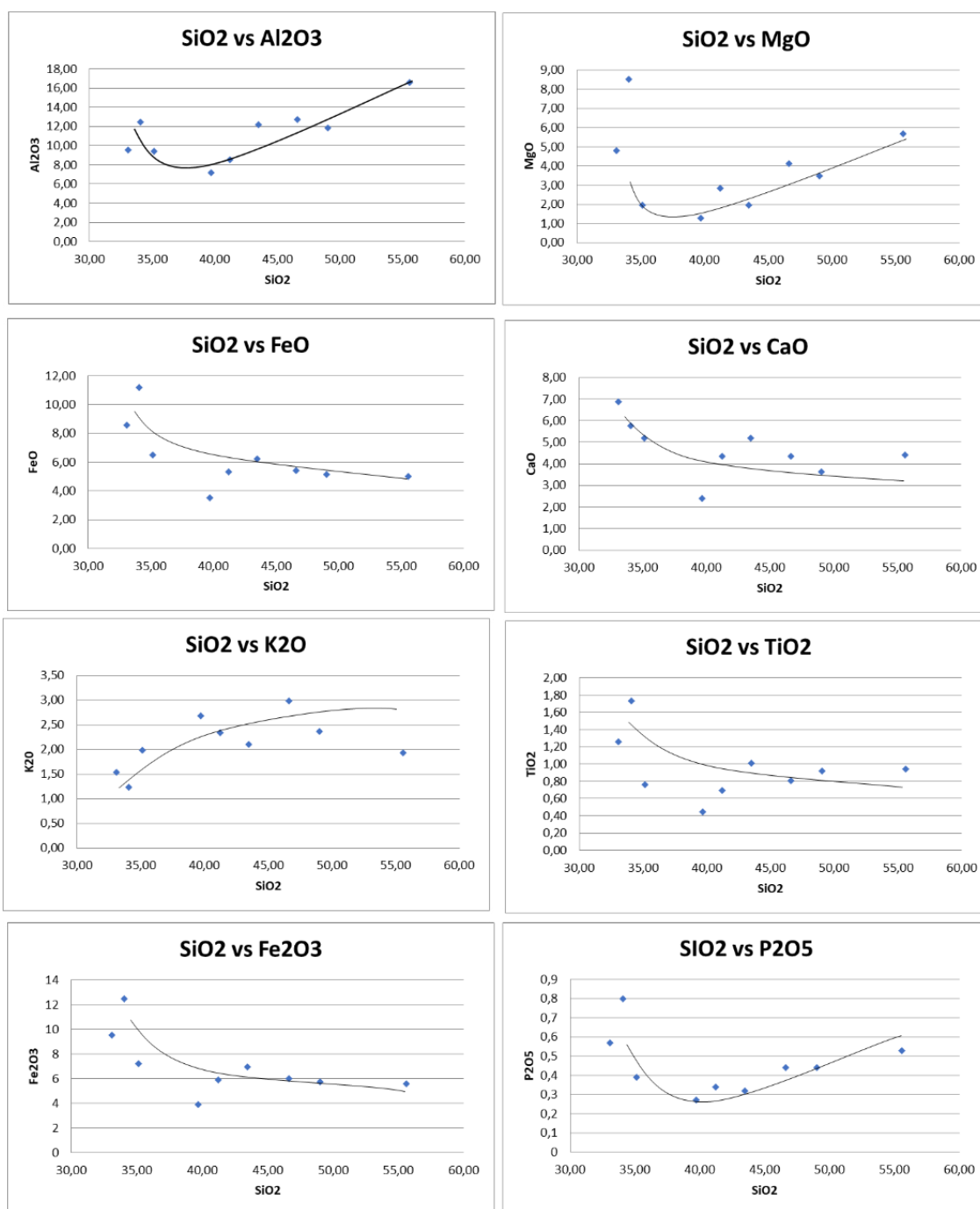
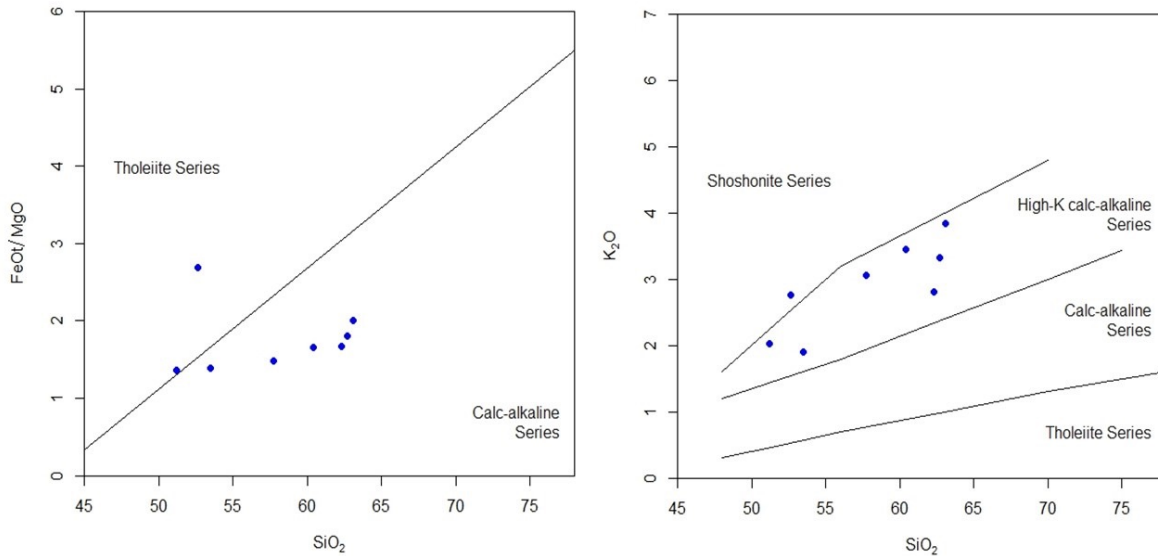


Figure 7. Diagrams of variation of [32] of the volcanic rocks of the Golero's Rhyolite analyzed.

#### 4.5 Type of magma

Miyashiro [34] and Peccerillo & Taylor [35], proposed to use a set of binary diagrams to distinguish the types of magmas (tholeiitic, calc-alkaline and alkaline), by the relationship that exists between some oxides as the FeO, MgO, K<sub>2</sub>O y el SiO<sub>2</sub>. The type of magma determined for the Rhyolite Unit of Golero based on the diagram proposed by [34], [35], is calc-alkaline (Fig. 8).



**Figure 8.-** Type of magma of Golero's Rhyolite Unit based on the elemental analyzes, using diagrams [34], [35]. It was determined that the basalts belonging to this unit come from a calc-alkaline magma.

#### 4.6 Tectonic site environment

For the determination of the tectonic environment in which the Golero's Rhyolite was formed, it was necessary to make the FeOt-MgO-Al<sub>2</sub>O<sub>3</sub> variation diagrams of [36]; the variation for andesitic rocks 10MnO-TiO<sub>2</sub>-10P<sub>2</sub>O<sub>5</sub> proposed by [37]; the variation Ti - Zr, proposed by [38], and the variation Rb - SiO<sub>2</sub> of [38].

#### 4.7 Diagram of variation FeOt-MgO-Al<sub>2</sub>O<sub>3</sub>

Pearce [39] proposed the triangular diagram with apices MgO, FeOt y Al<sub>2</sub>O<sub>3</sub>, where the tectonic limits for volcanic rocks of basic to intermediate, sub alkaline (tholeiitic and calc-alkaline) composition were defined, in which orogenic, continental, oceanic tectonic environments, among others, are distinguished.

In this diagram, the Golero's Rhyolite is found mostly in Orogenic environments, however, some rocks are found in the boundary between Ocean Island, Ocean Ridge and Floor (Ocean Rift Floor) (Fig. 9).

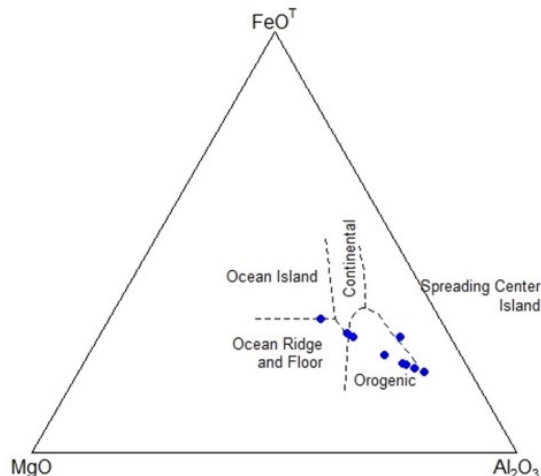


**Figure 9.-** FeOt-MgO-Al<sub>2</sub>O<sub>3</sub> variation diagram according to [39].

#### 4.8 Diagram of variation 10MnO-TiO<sub>2</sub>-10P<sub>2</sub>O<sub>5</sub>

Diagram proposed by [37] to discriminate by minor elements the tectonic environment of mafic and intermediate rocks (45 wt% <SiO<sub>2</sub> <54 wt %). The samples M-FGL 30, M-FGL 27-1 and M-FGL 26 of the Golero's Rhyolite belong to a tectonic environment of OIA (Oceanic Island Alkalic), possibly continental rift product (Fig. 10).

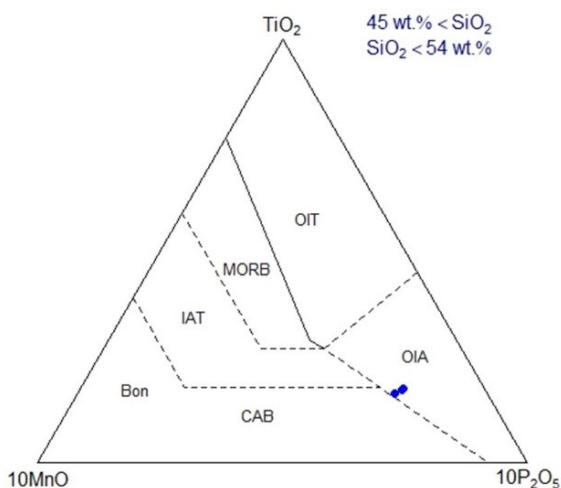


**Figure10.** Diagram of variation 10MnO-TiO<sub>2</sub>-10P<sub>2</sub>O<sub>5</sub> according to [37].

#### 4.9 Diagram of variation Ti – Zr

[38] in their study on the tectonic adjustments of basaltic rocks by means of trace elements, they determined the tectonic configurations of basaltic rocks using values of elements Ti, Zr.

Bearing in mind that when identifying the trace elements of basaltic rocks, it is possible to determine the original tectonic environment of an igneous system, the Ti versus Zr discrimination diagrams is used to establish their regional origin, using geochemical values of elements, such as Ti and Zr, according to [39].

The Golero's Rhyolite Unit presents percentages in ppm of Ti that several from 4316.28 to 10341.11, and Zr around 400, in the basalts described microscopically to which they were made X-ray fluorescence (FGL-30, FGL-21, FGL27 -1, FGL26-1, GFL11, FGL07 and FGL08), where the discrimination diagram shows that it was formed in an Intraplate zone (Fig. 11).

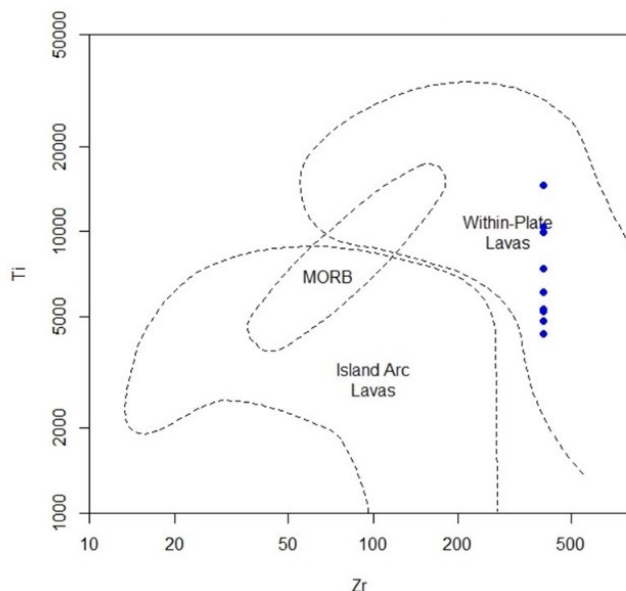


**Figure 11.** Diagram of Discrimination Ti - Zr according to [39].



#### 4.10 Diagram of variation Rb – SiO<sub>2</sub>

Discrimination Rb – SiO<sub>2</sub> proposed by [40], take into account trace elements of volcanic rocks for two tectonic environments (Intraplaca and mid-ocean ridges). Figure 12, shows values of Rb y SiO<sub>2</sub> from the Golero's Rhyolite Unit rocks where it is established that they were generated in a tectonic environment of Intraplaca, being congruent with the Tectonic discrimination diagram Ti-Zr by [37]. Keeping relation with the geological events proposed by [12], [41], which present an intrusive and effusive igneous activity product of the subduction of the Nazca plate under the South American craton, as illustrated in Fig. 12.

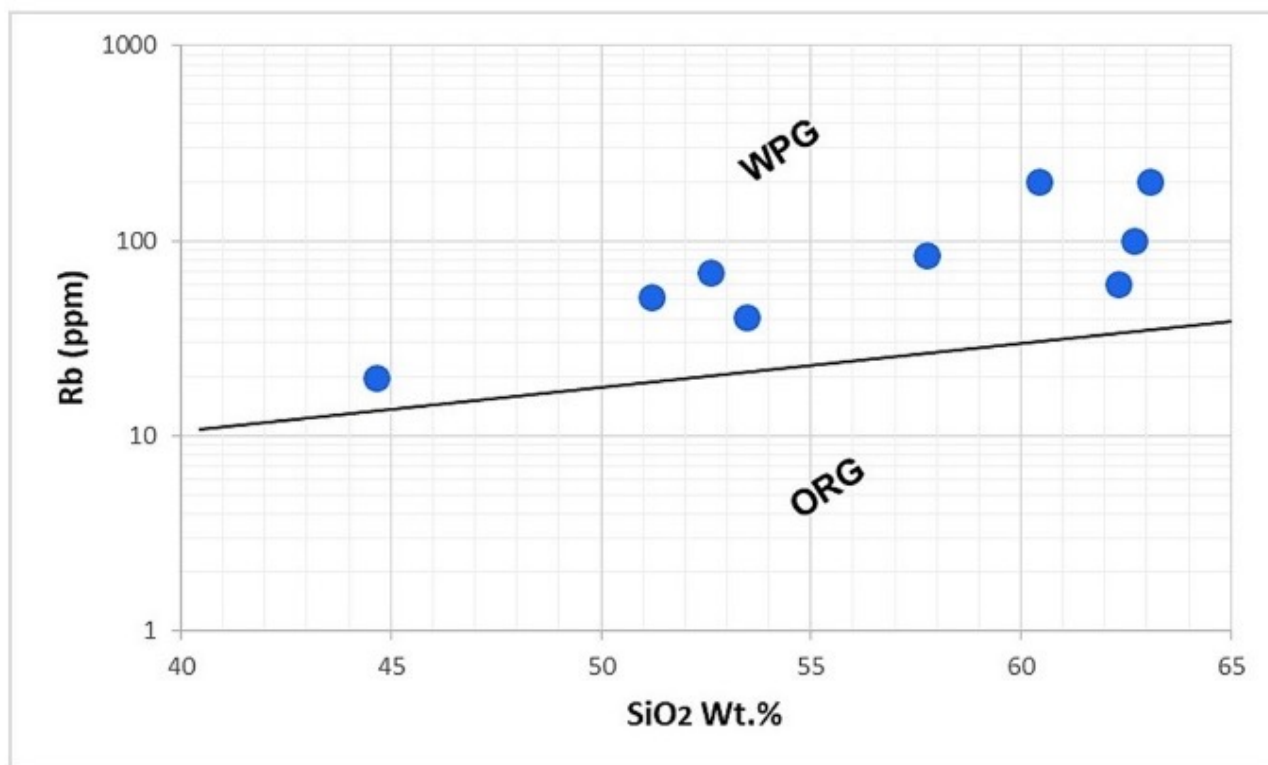


Figure 12. Diagram of Discrimination Rb – SiO<sub>2</sub>, proposed by [40].

## 5. CONCLUSIONS

The geological cartography reveals the geographical distribution of the lithologies of the Golero's Rhyolite Unit in the north of the city of Valledupar, with discordant contacts between the oldest and most recent rocks (Triassic Keratophire Porphyry, Guatapuri Formation, Alluvial Plain and Alluvial Fan).

Petrographically the volcanic rocks of the Golero's Rhyolite are igneous volcanic and volcano-sedimentary (ignimbrites), holocrystalline from greenish gray to dark gray, with distribution of grain size relatively inequigranular porphyry and serial inequigranular, of basic to intermediate composition, corresponding to basalts, andesites and dacites. These rocks have a high content of plagioclase (greater than 70%), quartz no greater than 15% and feldspar from 0 to 10%, with aphanitic and porphyritic texture, some xenoliths, and extreme epidotization.

The elements variation diagrams show that the volcanic rocks of the Golero's Rhyolite Unit present a tendency that suggests that they are part of the same magmatism and fractionation process with values in SiO<sub>2</sub> of 44.63 wt% up to 63.07wt% (basalts to dacites), with variations in the trends of the oxides as the SiO<sub>2</sub> content increases.

The rocks belonging to the Golero's Rhyolite Unit are of calc-alkaline affinity magmas formed in a tectonic environment of Intraplaca possibly influenced by continental oceanic rift islands.

## 6. ACKNOWLEDGEMENTS

The authors thank the engineer Jacqueline González and the X-ray Fluorescence Laboratory of the National University of Colombia for their support in carrying out the chemical analyzes. To the geological engineers Gustavo Arturo Cerchiaro Vásquez and Luisa Fernanda León Díaz, for their great collaborations and contributions in fieldwork. We also thank to members of the Research Group in Basic and Applied Geology of the Universidad Industrial de Santander for useful discussions. To all the people who otherwise supported and encouraged.

## 7. BIBLIOGRAPHIC REFERENCES

- [1] F. E. Audemard and F. A. Audemard, “Structure of the Mérida Andes, Venezuela: relations with the South America–Caribbean geodynamic interaction,” *Tectonophysics*, vol. 345, no. 1, pp. 1–26, 2002, doi: [https://doi.org/10.1016/S0040-1951\(01\)00218-9](https://doi.org/10.1016/S0040-1951(01)00218-9).
- [2] A. Taboada et al., “Geodynamics of the northern Andes,” *Tectonics*, vol. 19, no. 5, pp. 787–813, 2000.
- [3] B. T. Malfait and M. G. Dinkelman, “Circum-Caribbean Tectonic and Igneous Activity and the Evolution of the Caribbean Plate,” *GSA Bull.*, vol. 83, no. 2, pp. 251–272, Feb. 1972, doi: [10.1130/0016-7606\(1972\)83\[251:CTAIAA\]2.0.CO;2](https://doi.org/10.1130/0016-7606(1972)83[251:CTAIAA]2.0.CO;2).
- [4] J. Pindell, L. Kennan, W. Maresch, K. Stanek, G. Draper, and R. Higgs, “Plate-kinematics and crustal dynamics of circum-Caribbean arc-continent interactions: Tectonic controls on basin development in Proto-Caribbean margins,” *Spec. Pap. Geol. Soc. Am.*, vol. 394, pp. 7–52, Jan. 2005, doi: [10.1130/2005.2394\(01\)](https://doi.org/10.1130/2005.2394(01)).
- [5] C. N. G. Plata, “Estratigrafía y análisis de proveniencia de la Formación Los Indios, y su relación con la evolución tectónica de la Sierra Nevada de Santa Marta (Colombia),” Universidad Nacional de Colombia, 2017. [Online]. Available: <http://bdigital.unal.edu.co/59835/>
- [6] D. Quandt et al., “The geochemistry and geochronology of Early Jurassic igneous rocks from the Sierra Nevada de Santa Marta, NW Colombia, and tectono-magmatic implications,” *J. South Am. Earth Sci.*, vol. 86, pp. 216–230, 2018, doi: <https://doi.org/10.1016/j.jsames.2018.06.019>.
- [7] C. M. Tschanz, R. F. Marvin, and B. Cruz, “Geology of the Sierra Nevada de Santa Marta (Colombia)-Informe 1829,” INGEOMINAS, Bogotá, 1969.
- [8] C. Tschanz, A. Jimeno, J. Cruz, and U.S. Geological Survey, “Mapa Geológico de Reconocimiento de la Sierra Nevada de Santa Marta,” Bogotá D.C., Colombia, 1969.
- [9] G. Bayona et al., “Paleomagnetic data and K-Ar ages from Mesozoic units of the Santa Marta massif: A preliminary interpretation for block rotation and translations,” *J. South Am. Earth Sci.*, vol. 29, no. 4, pp. 817–831, 2010, doi: [10.1016/j.jsames.2009.10.005](https://doi.org/10.1016/j.jsames.2009.10.005).
- [10] F. Colmenares et al., “Geología De La Planchas 11, 12, 13, 14, 18, 19, 20, 21, 25, 26, 27, 33 Y 34,” Proyecto: “Evolución Geohistórica de la Sierra Nevada de Santa Marta”. Ministerio de Minas y Energía, Instituto Colombiano de Geología y Ministerio e Ingeominas, 2007. <http://recordcenter.sgc.gov.co/B12/23008010018162/documento/pdf/2105181621101000.pdf> (accessed Nov. 15, 2022).
- [11] L. Radelli, “Introducción al estudio de la geología y de la petrografía del Macizo de Santa Marta (Magdalena-Colombia),” *Geol. Colomb.*, vol. 2, no. 0 SE-Artículos, pp. 41–115, May 1962, [Online]. Available: <https://revistas.unal.edu.co/index.php/geocol/article/view/30349>

- [12] D. Barrero, "Geology of the Central Western Cordillera, west of Buga and Roldanillo, Colombia," Ministerio de Minas y Energia, Instituto Nacional de Investigaciones Geologico-Mineras, Bogotá D.C., Colombia, 1979. [Online]. Available: <http://books.google.com/books?id=G8IOAQAAIAAJ>
- [13] J. F. Toussaint and J. J. Restrepo, "Modelos orogénicos de tectónica de placas en los andes colombianos," *Bol. Cienc. Tierra*, vol. 1, pp. 1–47, 1976.
- [14] A. Estrada, *Geology and plate tectonics history of the Colombian Andes*. Stanford University, 1972.
- [15] C. Macla and J. Mojica, "Nuevos puntos de vista sobre el magmatismo Triasico Superior (Fm. Saldana), Valle Superior del Magdalena, Colombia," *Zbl. Geol. Palaont.* 1, pp. 243–251, 1981.
- [16] A. Cardona et al., "Permian to Triassic I to S-type magmatic switch in the northeast Sierra Nevada de Santa Marta and adjacent regions, Colombian Caribbean: Tectonic setting and implications within Pangea paleogeography," *J. South Am. Earth Sci.*, vol. 29, no. 4, pp. 772–783, 2010, doi: 10.1016/j.jsames.2009.12.005.
- [17] A. Piraquive, A. Kammer, A. Von Quadt, and M. Bernet, "Permo-Triassic evolution in the Sierra Nevada de Santa Marta, from the Alleghenides collision to Pangaea break-up," *Universidad Nacional de Colombia - Université Grenoble-Alpes*, 2016.
- [18] A. Cardona et al., "Tectonomagmatic setting and provenance of the Santa Marta Schists, northern Colombia: Insights on the growth and approach of Cretaceous Caribbean oceanic terranes to the South American continent," *J. South Am. Earth Sci.*, vol. 29, no. 4, pp. 784–804, 2010, doi: 10.1016/j.jsames.2009.08.012.
- [19] J. Duque-Trujillo, "Geocronología (U/Pb y 40Ar/39Ar) y geoquímica de los intrusivos paleógenos de la Sierra Nevada de Santa Marta y sus relaciones con la tectónica del Caribe y el arco magmático circun-caribeño," *Universidad Nacional Autónoma de México*, 2009.
- [20] J. Duque-Trujillo, T. Orozco-Esquivel, C. Sánchez, and A. Cárdenas-Rozo, "Paleogene Magmatism of the Maracaibo Block and Its Tectonic Significance," *Geol. Tectonics Northwest. South Am.*, pp. 551–561, 2019, doi: [https://doi.org/10.1007/978-3-319-76132-9\\_7](https://doi.org/10.1007/978-3-319-76132-9_7).
- [21] C. Tschanz, R. Marvin, J. Cruz B., H. Mehnert, and G. Cebula, "Geologic Evolution of the Sierra Nevada de Santa Marta, Northeastern Colombia," *GSA Bull.*, vol. 85, no. 2, pp. 273–284, Feb. 1974, doi: 10.1130/0016-7606(1974)85<273:GEOTSN>2.0.CO;2.
- [22] E. Cortes Castillo, "Análisis Petrogenético de las Denominadas 'Anortositas' Aflorantes en la Vertiente Occidental de La Sierra Nevada de Santa Marta - Sector Río Sevilla - El Palmor (Colombia)," *Universidad Nacional de Colombia*, 2013. [Online]. Available: <http://www.bdigital.unal.edu.co/39643/>
- [23] O. Ordóñez, M. Pimentel, and R. de Moraes, "Granulitas de los mangos, un fragmento grenvilliano en la parte oriental de la Sierra Nevada de Santa Marta," *Rev. la Acad. Colomb. Ciencias Exactas, Fis. y Nat.*, vol. 26, no. 99, pp. 169–179, Jul. 2002.
- [24] F. Lascarro-Navarro, M. Lozada-Molina, D. Manco-Jaraba, and E. Rojas-Martínez, "Análisis estructural y morfotectónico al norte de Valledupar-Cesar, Colombia: contribución a los estudios de peligrosidad sísmica de la Falla Río Seco," *Ingeniare. Rev. Chil. Ing.*, vol. 28, no. 2, pp. 255–267, 2020, doi: 10.4067/s0718-33052020000200255.



- [25] K. M. Teheran Ochoa and L. C. Tapia Vela, “Análisis neotectónico de la falla río seco, ciudad de Valledupar, Cesar,” *Investig. e Innovación en Ing.*, vol. 6, no. 1 SE-Artículos, pp. 40–57, Jan. 2018, doi: 10.17081/invin-no.6.1.2774.
- [26] A. Arias and C. Morales, *Mapa geológico generalizado del departamento del Cesar - Memoria explicativa*. Bogotá D.C., Colombia: Instituto Nacional de Investigaciones Geológico Mineras (INGEOMINAS) ;, 1999. Accessed: Sep. 21, 2020. [Online]. Available: <https://catalogo.sgc.gov.co/cgi-bin/koha/opac-detail.pl?biblionumber=14212>
- [27] R. Le Maitre, A. Streckeisen, B. Zanettin, M. Le Bas, B. Bonin, and P. Bateman, *Igneous Rocks: A Classification and Glossary of Terms: Recommendations of the International Union of Geological Sciences Subcommittee on the Systematics of Igneous Rocks*, 2nd ed. Cambridge: Cambridge University Press, 2002. doi: DOI: 10.1017/CBO9780511535581.
- [28] R. Kretz, “Symbols for rock-forming minerals,” *Am. Mineral.*, vol. 68, no. 1–2, pp. 277–279, 1983, [Online]. Available: [http://www.minsocam.org/ammin/AM68/AM68\\_277.pdf](http://www.minsocam.org/ammin/AM68/AM68_277.pdf)
- [29] A. Streckeisen, “Classification of the common igneous rocks by means of their chemical composition; a provisional attempt,” p. shefte. 1, Pages 1-15. 1976., 1976.
- [30] E. A. K. Middlemost, “Naming materials in the magma/igneous rock system,” *Earth-Science Rev.*, vol. 37, no. 3, pp. 215–224, 1994, doi: [https://doi.org/10.1016/0012-8252\(94\)90029-9](https://doi.org/10.1016/0012-8252(94)90029-9).
- [31] N. L. Bowen, “The Later Stages of the Evolution of the Igneous Rocks,” *J. Geol.*, vol. 23, no. S8, pp. 1–91, 1915, doi: 10.1086/622298.
- [32] A. Harker, *The natural history of igneous rocks*. London, 1909.
- [33] N. L. Bowen, “The Evolution of the Igneous Rocks,” *Nature*, vol. 124, no. 3126, pp. 474–475, 1929, doi: 10.1038/124474a0.
- [34] A. Miyashiro, “Volcanic rock series in island arcs and active continental margins,” *Am. J. Sci.*, vol. 274, no. 4, pp. 321–355, Apr. 1974, doi: 10.2475/ajs.274.4.321.
- [35] A. Peccerillo and S. R. Taylor, “Geochemistry of eocene calc-alkaline volcanic rocks from the Kastamonu area, Northern Turkey,” *Contrib. to Mineral. Petrol.*, vol. 58, no. 1, pp. 63–81, 1976, doi: 10.1007/BF00384745.
- [36] M. W. Ali-Bik and S. S. Gabr, “Spectral analyses, geology and petrology of the Gulf of Suez rift-related Oligo-Miocene basalts at Abu Zenima area, west central Sinai, Egypt,” *Egypt. J. Remote Sens. Sp. Sci.*, vol. 25, no. 1, pp. 85–96, 2022, doi: <https://doi.org/10.1016/j.ejrs.2022.01.002>.
- [37] E. D. Mullen, “MnO/TiO<sub>2</sub>/P<sub>2</sub>O<sub>5</sub>: a minor element discriminant for basaltic rocks of oceanic environments and its implications for petrogenesis,” *Earth Planet. Sci. Lett.*, vol. 62, no. 1, pp. 53–62, 1983, doi: [https://doi.org/10.1016/0012-821X\(83\)90070-5](https://doi.org/10.1016/0012-821X(83)90070-5).
- [38] J. A. Pearce and J. R. Cann, “Tectonic setting of basic volcanic rocks determined using trace element analyses,” *Earth Planet. Sci. Lett.*, vol. 19, no. 2, pp. 290–300, 1973, doi: [https://doi.org/10.1016/0012-821X\(73\)90129-5](https://doi.org/10.1016/0012-821X(73)90129-5).

- [39] T. H. Pearce, B. E. Gorman, and T. C. Birkett, "The relationship between major element chemistry and tectonic environment of basic and intermediate volcanic rocks," *Earth Planet. Sci. Lett.*, vol. 36, no. 1, pp. 121–132, 1977, doi: [https://doi.org/10.1016/0012-821X\(77\)90193-5](https://doi.org/10.1016/0012-821X(77)90193-5).
- [40] J. A. Pearce, N. B. W. Harris, and A. G. Tindle, "Trace Element Discrimination Diagrams for the Tectonic Interpretation of Granitic Rocks," *J. Petrol.*, vol. 25, no. 4, pp. 956–983, Nov. 1984, doi: [10.1093/petrology/25.4.956](https://doi.org/10.1093/petrology/25.4.956).
- [41] J. Toussaint and J. Restrepo, *The Colombian Andes During Cretaceous Times*. 1994. doi: [https://doi.org/10.1007/978-3-322-85472-8\\_2](https://doi.org/10.1007/978-3-322-85472-8_2).